Electronic structure of the Si(111) $\sqrt{3}\times\sqrt{3}R30°$-B surface

H. Q. Shi, M. W. Radny, and P. V. Smith*
School of Mathematical and Physical Sciences, The University of Newcastle, Callaghan, NSW, Australia, 2308
(Received 3 April 2002; published 30 August 2002)

The plane-wave pseudopotential density functional theory (DFT) package FHI98MD has been used to optimize the geometry of the Si(111) $\sqrt{3}\times\sqrt{3}R30°$-B($S_5$) configuration. The resultant geometry has been found to be in excellent agreement with recent experimental results. By calculating the band structure for the B(S_5) configuration and carefully analyzing the nature of the wave functions in the vicinity of the Fermi energy, we have been able to identify the surface states along the various symmetry directions of the surface Brillouin zone (SBZ). The overall dispersion of both the occupied and unoccupied surface state bands is found to be in excellent agreement with the angle-resolved photoemission data. The theoretical calculations also predict the occurrence of two occupied surface state bands at the Γ and M points of the SBZ. The splitting of these bands is predicted to be 0.27 eV and 0.35 eV, respectively, in good agreement with experiment.

DOI: 10.1103/PhysRevB.66.085329 PACS number(s): 68.35.Bs, 73.20.−r

I. INTRODUCTION

The chemisorption of group-III elements (B, Al, Ga, and In) on silicon surfaces has attracted a great deal of attention in semiconductor surface science.[1] Of particular interest in these studies has been the modification of the atomic and electronic structure of the Si(111) surface produced by the chemisorption of boron. This is primarily due to the unexpected behavior of boron atoms chemisorbed on the Si(111) surface.

Group III elements chemisorbed on the Si(111) surface are expected to saturate the dangling bonds and completely passivate this chemically active surface. There are two preferred chemisorption sites for trivalent elements on the Si(111) surface: the T_4 and H_3 sites. The adatom T_4 site locates the chemisorbed atom in the threefold-coordinated site directly above a second-layer silicon atom, while the H_3 adatom site locates the chemisorbed atom in the threefold "hollow" site directly above a fourth-layer silicon atom. Adatoms placed on the ideal Si(111)1×1 surface at the T_4 or H_3 sites form a $\sqrt{3}\times\sqrt{3}R30°$ layer above the truncated 1x1 silicon surface atoms. Reviews of the early work on the interaction of Al, Ga, and In with the Si(111) surface have been provided by Uhrberg and Hansson[2] and Kono.[3]

The first angle-resolved photoemission (ARUPS) measurements for these systems was made on the Si(111) $\sqrt{3}\times\sqrt{3}R30°$-Al surface by Hansson *et al.*[4,5] Probing in different azimuthal directions they obtained two different surface state energies at the M point of the surface Brillouin zone (SBZ). This led them to predict the existence of two occupied surface-state bands with a bandwidth of 0.4 eV. Subsequently Uhrberg *et al.*[6] carried out a more detailed study which confirmed the existence of the two different M point energies and predicted a bandwidth of 0.65 eV. The two occupied surface state bands, however, remained unresolved. Resolution of these two bands for the $\sqrt{3}\times\sqrt{3}R30°$ surface induced by Al was achieved using ARUPS by Kinoshita *et al.*[7] in 1985. The Si(111) $\sqrt{3}\times\sqrt{3}R30°$-Ga surface[8,9] and the Si(111) $\sqrt{3}\times\sqrt{3}R30°$-In surface[9–11] have also been studied using ARUPS. The ARUPS spectra of the three surfaces (Al, Ga, and In) were found to be almost indistinguishable. The dispersions of the unoccupied surface-state bands determined by inverse photoemission were also found to be very similar.[12]

Density functional theory calculations of the Si(111) $\sqrt{3}\times\sqrt{3}R30°$-Al surface by Northrup[13] produced two bands with a splitting at the M point in good agreement with experiment. Both the T_4 and H_3 sites were found to exhibit similar dispersions. Chemisorption at the T_4 sites, however, was found to be more energetically favorable than chemisorption at the H_3 sites by 0.3 eV/atom. Calculations by Nicholls *et al.*[11] for the Si(111) $\sqrt{3}\times\sqrt{3}R30°$-In surface also predicted two occupied surface-state bands for both the T_4 and H_3 chemisorption models in agreement with experiment. The H_3 model, however, was determined to be 0.2 eV/atom less stable than the T_4 model. First-principles total-energy calculations for the Si(111) $\sqrt{3}\times\sqrt{3}R30°$-Ga surface have predicted analogous dispersions to the Al and In surfaces with chemisorption at the T_4 sites again being preferred by 0.38 eV/atom.[12,14]

The chemisorption of boron induces a $\sqrt{3}\times\sqrt{3}R30°$ reconstruction of the Si(111) surface at 0.33 ML coverage analogous to the other group-III elements (Al, Ga and In). In this case, however, the experimental data[15–17] suggested that the boron atoms would chemisorb at either the T_4 adatom sites or in the second-layer positions, the so-called S_5 sites, directly beneath the T_4 sites. Total-energy calculations confirmed these predictions and determined the S_5 site to be more stable than the T_4 site by ~1.0 eV per $\sqrt{3}\times\sqrt{3}$ surface unit cell.[16–18] It is believed that the stability of the B(S_5) structure is due to the shortness of the Si-B bonds which makes it easy for the boron atoms to occupy the S_5 substitutional subsurface positions and acquire charge from the neighboring silicon atoms.

The electronic structure of the B(S_5)-reconstructed Si(111) surface was studied by Higashiyama *et al.* using ARUPS.[19] They found two dispersive surface states below the Fermi energy with a splitting at the M point of 0.3 eV. An earlier study by Kaxiras *et al.*[18] indicated only a single occupied surface state below the Fermi energy of the

 ©2002 The American Physical Society

TABLE I. The difference in energy (in eV) of the $B(S_5)$, $B(T_4)$, and $B(H_3)$ configurations obtained from our plane-wave pseudopotential FHI98MD calculations. Other theoretical values are given for comparison.

Energy difference	Present calculation	Ref. 17	Ref. 23	Ref. 24
$E(B{:}T_4)-E(B{:}S_5)$	1.05	1.0	1.1($Si_{27}H_{26}$) 1.05($Si_{109}H_{78}$)	1.75
$E(B{:}H_3)-E(B{:}T_4)$	1.40	1.1		

$Si(111)\sqrt{3}\times\sqrt{3}R30°$-B surface. Kaxiras *et al.* also calculated a band structure for the $B(S_5)$ surface using density functional theory. The theoretical results (which are only presented for part of the SBZ) were shown to be in reasonable agreement with the experimental data. While some splitting at the M point was predicted by these theoretical calculations, this was much smaller than that observed by Higashiyama *et al.*[19]

The aim of this paper is to use an accurate first principles method to calculate the electronic structure of the $B(S_5)$ surface and to compare this band structure with the experimental results. We will also investigate the difference between the electronic structure of the boron chemisorbed Si(111) surface and those of the other group-III elements absorbed on the Si(111) surface.

II. METHOD AND PROCEDURE

Our calculations have been carried out using an *ab initio* density functional theory (DFT) method for periodic slabs and employing the local density approximation (LDA) for electron exchange and correlation. The first-principles code FHI98MD (Ref. 20) was used to carry out the geometry optimization surface calculations. Within this method, the Kohn-Sham equations were solved using plane waves with kinetic energies up to 18 Ry and 6 special **k** points in the irreducible part of the SBZ of the $Si(111)\sqrt{3}\times\sqrt{3}$ cell. Our slab consisted of 8 layers of silicon with 3 hydrogen atoms directly below the bottom silicon atoms to saturate the bulk dangling bonds of each surface unit cell. A vacuum region of ~ 11 a.u. was also incorporated to ensure inclusion of the dipole correction. The top four layers of the slab were allowed to vary and the minimum-energy structure was found by minimizing the forces using the Hellmann-Feynman theorem. Norm conserving pseudopotentials by Hamann[21] were employed for silicon and boron, and the pseudopotential of hydrogen was that provided by Fuchs.[22]

III. RESULTS AND DISCUSSION

A. Energy

The relative energies of the $B(T_4)$, $B(S_5)$, and $B(H_3)$ optimized geometries obtained from the FHI98MD plane-wave pseudopotential calculations are presented in Table I. Also given are the corresponding values obtained from the DFT calculations of Lyo *et al.*[17] and the cluster calculations of Zavodinsky *et al.*[23] and Wang *et al.*[24] The total energy of the $B(S_5)$ configuration is predicted by the FHI98MD calculations to be 1.05 eV per surface unit cell lower than that of the $B(T_4)$ configuration. This result is in excellent agreement with the value of 1.0 eV obtained by Lyo *et al.*[17] and the values of 1.1 eV and 1.05 eV calculated by Zavodinsky *et al.*[23] using different-sized clusters. These results confirm that the $B(S_5)$ geometry is more stable than the $B(T_4)$. The total energy of the $B(H_3)$ topology is predicted by the FHI98MD calculations to be 1.40 eV per surface unit cell greater than that of the $B(T_4)$ topology. This is consistent with the value of 1.1 eV that one can determine from the plane-wave DFT calculations of Lyo *et al.*[17] It follows that chemisorption at the threefold-coordinated H_3 on-top site is less energetically favorable than chemisorption at the analogous T_4 site. The preferred site for boron chemisorption, however, is clearly the subsurface S_5 site.

B. Geometry

The topology of the optimized $B(S_5)$ structure obtained from our geometry optimization calculations is shown in Fig 1. The calculated atomic relaxations and bond lengths of the various atoms are presented in Table II. The boron atom at the subsurface S_5 position $[B(S_5)]$ is bonded to four silicon atoms: the three first-layer atoms at distances of 2.03 Å, 2.12 Å, and 2.08 Å and the underlying third-layer atom. This latter atom is predicted to be at a distance of 1.98 Å, in excellent agreement with the recent experimental value of 1.98 ± 0.04 Å.[25] The distance between the $Si(T_4)$ adatom and the $B(S_5)$ atom is 2.18 Å. The position of the third-layer silicon atom is seen to be almost unaffected by the presence of the chemisorbed $B(S_5)$ atom. This is in agreement with other theoretical calculations[17,26] but disagrees with the low

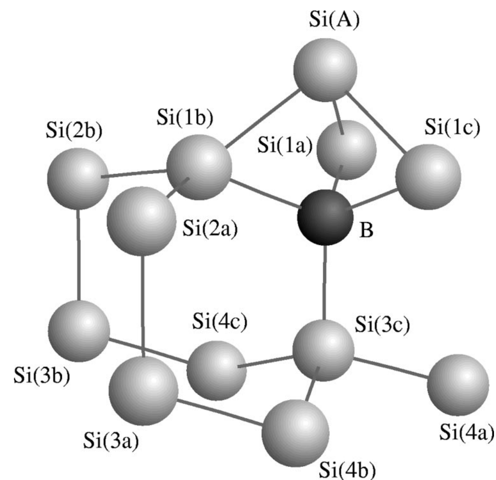

FIG. 1. The topology of the $Si(111)\sqrt{3}\times\sqrt{3}R30°$-$B(S_5)$ configuration.

TABLE II. The atomic relaxations and bond lengths (in Å) of our optimized geometry for the Si(111) $\sqrt{3}\times\sqrt{3}R30°$-B($S_5$) configuration. The z coordinate is normal to the surface and r lies in the x-y plane. Other theoretical and experimental values are given for comparison.

Geometry	Present calculation	Ref. 25	Ref. 27	Ref. 17	Ref. 28	Ref. 26	Ref. 26
$\Delta z_{Si(A)}$	0.21		0.25±0.1	0.28		0.24	0.19
$\Delta z_{Si(1a)}$	−0.45						
$\Delta z_{Si(1b)}$	−0.38		−0.30±0.1	−0.30	−0.17±0.2	−0.41	−0.40
$\Delta z_{Si(1c)}$	−0.38						
Δz_{B}	−0.42		−0.50±0.1	−0.37		−0.39	−0.38
$\Delta z_{Si(3a)}$	−0.04						
$\Delta z_{Si(3b)}$	−0.03	0.0					
$\Delta z_{Si(3c)}$	−0.08		−0.34±0.1	−0.06		−0.02	−0.04
$\Delta r_{Si(1a)}$	−0.30						
$\Delta r_{Si(1b)}$	−0.29		−0.30±0.2	−0.26	−0.26±0.01	−0.24	−0.23
$\Delta r_{Si(1c)}$	−0.27						
$d_{Si(A)\text{-}Si(1a)}$	2.380						
$d_{Si(A)\text{-}Si(1b)}$	2.350		2.336	2.457		2.435	2.412
$d_{Si(A)\text{-}Si(1c)}$	2.359						
$d_{Si(A)\text{-}B}$	2.184	2.14±0.13	2.320	2.216		2.202	2.179
$d_{Si(1a)\text{-}B}$	2.025						
$d_{Si(1b)\text{-}B}$	2.117	2.21±0.13	2.154	2.216		2.116	2.137
$d_{Si(1c)\text{-}B}$	2.083						
$d_{Si(3c)-B}$	1.984	1.98±0.04	2.190	2.042		1.973	1.972
$d_{Si(1a)\text{-}Si(1b)}$	3.310						
$d_{Si(1b)\text{-}Si(1c)}$	3.329		3.326	3.390	3.390	3.414	3.431
$d_{Si(1c)\text{-}Si(1a)}$	3.312						
$d_{Si(4a)\text{-}B}$	3.509						
$d_{Si(4b)\text{-}B}$	3.471	3.53±0.09					
$d_{Si(4c)\text{-}B}$	3.507						
$z_{Si(5)}\text{-}z_{Si(A)}$	5.02	5.20±0.20					
$z_{Si(2a)}\text{-}z_{B}$	0.40						
$z_{Si(2b)}\text{-}z_{B}$	0.41	0.49±0.35					
$z_{Si(3a)}\text{-}z_{B}$	1.95						
$z_{Si(3b)}\text{-}z_{B}$	1.94	1.90±0.16					

energy electron diffraction (LEED) analysis of Huang *et al.*[27] which predicts significant displacement of the third layer silicon atom.

Our results are seen to be in excellent agreement with the recent photoelectron diffraction data obtained by Baumgartel *et al.*[25] Our calculated results are also in very good agreement with the values derived from the LEED analysis of Huang *et al.*[27] with the exception of the vertical relaxation of the third-layer silicon atom ($\Delta z_{Si(3c)}$), and the associated bond length $d_{Si(3c)\text{-}B}$. We believe that these two latter values, which are at variance with the recent photoelectron diffraction results, are probably a result of ignoring any relaxations below the third layer in the LEED fitting procedure. The values obtained from the current plane-wave pseudopotential calculations are clearly in excellent overall agreement with the Hartree-Fock–density-functional-theory (HF-DFT) cluster calculations of Wang *et al.*[26] and the pseudopotential local-density-functional plane-wave calculations of Lyo *et al.*[17]

The topology of the optimized B(T_4) structure is shown in Fig. 2 and the calculated atomic relaxations and bond lengths presented in Table III. The boron atom at the threefold-coordinated T_4 adatom position [B(T_4)] is bonded to three first layer silicon atoms at distances of 2.07 Å, 2.08 Å, and 2.07 Å, respectively. The distances between the Si(S_5) atom and the first layer silicon atoms are 2.31 Å, 2.40 Å and 2.38 Å, respectively, while the length of the bond between the Si(S_5) atom and the underlying third-layer silicon atom is only 2.22 Å. The distance between the B(T_4) adatom and the Si(S_5) atom is even smaller at 2.10 Å.

The calculated results are again observed to be in very good agreement with the plane-wave DFT calculations of Lyo *et al.*[17] and the HF-DFT cluster calculations of Wang *et al.*[26] The only really significant difference occurs for the first layer silicon atoms where the vertical relaxations predicted by the cluster calculations are of the opposite sign to our plane-wave values. This may simply be a cluster size effect as the clusters employed by Wang *et al.*[26] were of

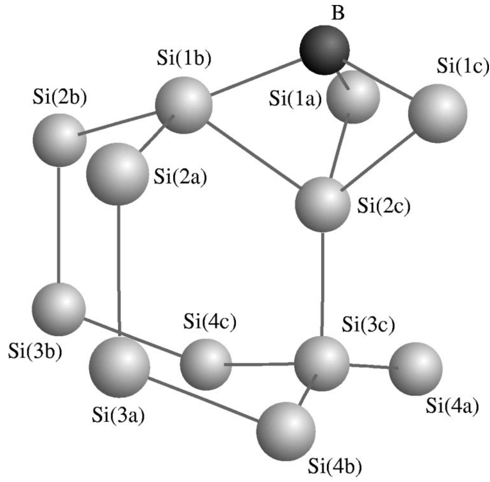

FIG. 2. The topology of the Si(111) $\sqrt{3}\times\sqrt{3}R30°$-B($T_4$) configuration.

necessity quite small. Such differences were not observed, however, for the B(S_5) topology. In general, the B(T_4) cluster calculations predict the boron atom and the first- and second-layer silicon atoms to lie below the corresponding plane-wave values.

TABLE III. The atomic relaxations and bond lengths (in Å) of our optimized geometry for the Si(111) $\sqrt{3}\times\sqrt{3}R30°$-B($T_4$) topology. The z coordinate is normal to the surface and r lies in the x-y plane. Other theoretically derived values are given for comparison.

Geometry	Present calculation	Ref. 17	Ref. 26	Ref. 26
Δz_B	0.05	0.07	−0.06	−0.03
$\Delta z_{Si(1a)}$	0.02			
$\Delta z_{Si(1b)}$	0.12	−0.01	−0.15	−0.19
$\Delta z_{Si(1c)}$	0.12			
$\Delta z_{Si(2a)}$	0.25			
$\Delta z_{Si(2b)}$	0.25			
$\Delta z_{Si(2c)}$	−0.50	−0.52	−0.58	−0.60
$\Delta z_{Si(3a)}$	0.16			
$\Delta z_{Si(3b)}$	0.17			
$\Delta z_{Si(3c)}$	−0.38	−0.39	−0.40	−0.41
$\Delta r_{Si(1a)}$	−0.29			
$\Delta r_{Si(1b)}$	−0.25	−0.24	−0.20	−0.21
$\Delta r_{Si(1c)}$	−0.25			
$d_{B\text{-}Si(1a)}$	2.070			
$d_{B\text{-}Si(1b)}$	2.077	2.154	2.192	2.214
$d_{B\text{-}Si(1c)}$	2.074			
$d_{B\text{-}Si(2c)}$	2.097	2.158	2.086	2.138
$d_{Si(1b)\text{-}Si(2a)}$	2.387			
$d_{Si(1b)\text{-}Si(2b)}$	2.406			
$d_{Si(1b)\text{-}Si(2c)}$	2.400	2.368	2.348	2.334
$d_{Si(2a)\text{-}Si(3a)}$	2.415			
$d_{Si(2b)\text{-}Si(3b)}$	2.415			
$d_{Si(2c)\text{-}Si(3c)}$	2.216	2.231	2.168	2.153
$d_{Si(1a)\text{-}Si(1b)}$	3.341			
$d_{Si(1b)\text{-}Si(1c)}$	3.387	3.434	3.483	3.470
$d_{Si(1c)\text{-}Si(1a)}$	3.335			

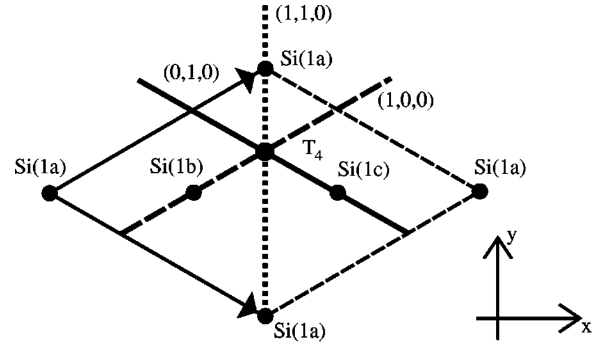

FIG. 3. Schematic of the Si(111) $\sqrt{3}\times\sqrt{3}R30°$ surface unit cell indicating the T_4 adatom site and the three planes that have been employed to analyze the wave functions.

C. Electronic structure

1. Si(111) $\sqrt{3}\times\sqrt{3}$R30 °-B(S_5)

To identify the electronic surface states we have calculated the function $\rho_{n\mathbf{k}}(z)$ defined by

$$\rho_{n\mathbf{k}}(z)=\int_{SUC}|\Psi_{n\mathbf{k}}(x,y,z)|^2dxdy,$$

where x and y lie in the surface plane, z is out of the surface, and the integration is performed over the surface unit cell (SUC). This quantity gives the z dependence of the modulus of the wave function squared averaged over the surface unit cell. To determine the actual nature of the various surface states we have plotted charge density contour plots for three different symmetry planes within the surface unit cell. These planes are oriented at 120° with respect to each other and include the T_4, S_5, and Si($1c$), the T_4, S_5, and Si($1b$), and the T_4, S_5, and Si($1a$) sites, respectively (see Fig. 3). Their Miller indices, defined in terms of the reciprocal lattice vectors of the $\sqrt{3}\times\sqrt{3}R30°$ surface unit cell, are (0,1,0), (1,0,0), and (1,1,0), respectively. To examine the **k** dependence of the surface-state bands, the $\rho_{n\mathbf{k}}(z)$ were calculated for 20 **k** points along the Γ-K-M-Γ directions of the SBZ. This enabled the surface states at each **k** point to be identified and plotted on the overall band structure.

An enlarged view of the electronic structure that we have obtained for the Si(111) $\sqrt{3}\times\sqrt{3}R30°$-B($S_5$) surface in the vicinity of the valence-band maximum (VBM) is shown in Fig. 4. The theoretically predicted unoccupied surface states are indicated by the solid triangles and diamonds. Only the lowest-energy unoccupied surface states have been indicated for simplicity. The experimental results of Grehk *et al.*[29] obtained using KRIPES (**k**-resolved inverse photoelectron spectroscopy) are shown as open triangles. These values have been shifted by a constant amount to match the theoretically predicted value at the M point. This shift is required because of the neglect of self-energy effects in the standard LDA theory. The agreement between the theoretical results (solid triangles) and the experimental data of Grehk *et al.* (open triangles) is clearly excellent with the theoretical calculations accurately predicting both the overall bandwidth and the initial upward dispersion of this unoccupied surface-

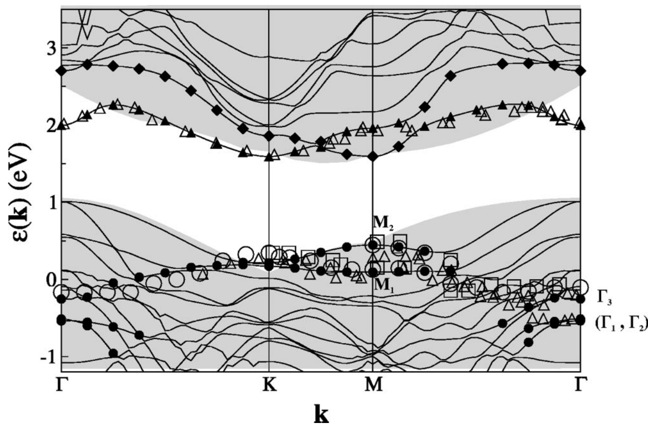

FIG. 4. The electronic structure of the $B(S_5)$ configuration in the vicinity of the VBM. The solid circles, triangles, and diamonds indicate the theoretically predicted electronic surface states. The open circles and squares represent the experimental data of Higashiyama *et al.* (Ref. 19). The open triangles indicate the experimental results of Grehk *et al.* (Ref. 29).

state band along the Γ-*K* and Γ-*M* directions. Previous work by Kaxiras *et al.*[18] had predicted that this band would simply disperse downward from the Γ point along both symmetry directions. Charge density plots for this unoccupied surface state band at the Γ, *K* and *M* points of the SBZ are presented in Fig. 5. Also plotted in this figure are the corresponding $\rho_{n\mathbf{k}}(z)$. It is clear that these unoccupied surface states are dangling bond states associated with the Si adatom of the $B(S_5)$ configuration. Charge density contour plots for the unoccupied surface states indicated in Fig. 4 by the solid diamonds are shown in Fig. 6 for the Γ, *K*, and *M* points of the SBZ. These empty states are clearly quite different to the dangling bond states and involve coupling between the silicon adatom $[\mathrm{Si}(T_4)]$ and the underlying boron atom in the second layer $[B(S_5)]$.

The theoretically predicted surface states for the valence band are shown in Fig. 4 as the solid circles. At the Γ point,

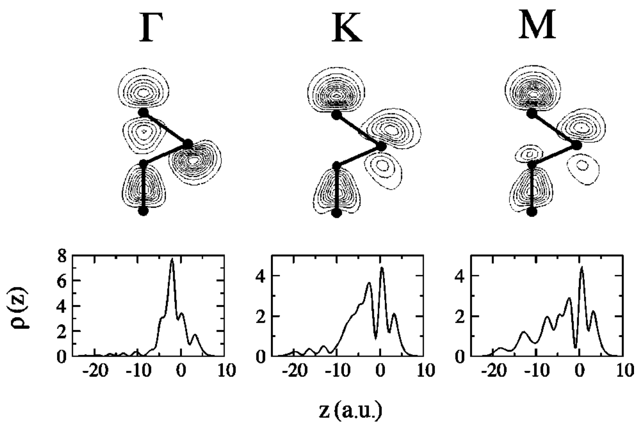

FIG. 5. Charge density contour plots and the corresponding $\rho_{n\mathbf{k}}(z)$ for the empty dangling bond surface states for the $B(S_5)$ configuration at the Γ, *K*, and *M* points of the surface Brillouin zone. The contour plots are for the (0,1,0) plane. $z=0$ corresponds to the position of the first-layer atoms in the unrelaxed surface and the bottom silicon layer is at $z=-19.1$ a.u..

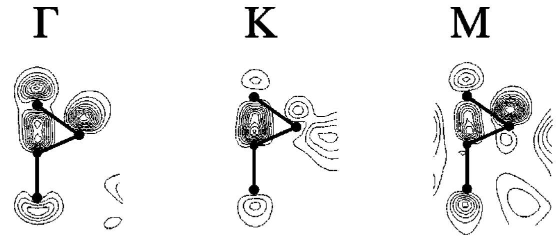

FIG. 6. Charge density contour plots for the empty surface states indicated by the solid diamonds in Fig. 4 for the $B(S_5)$ configuration at the Γ, *K*, and *M* points of the SBZ. The contour plots are for the (0,1,0) plane.

there is an upper surface state (Γ_3) lying 1.26 eV below the valence-band maximum and two essentially degenerate lower-lying states (Γ_1, Γ_2) positioned 1.53 eV below the VBM. The upper band increases gradually in energy along the Γ-*K* direction but initially decreases along Γ-*M*. The lower band decreases in energy and splits into two along the Γ-*K* and Γ-*M* directions. At the K point, our calculation predicts the occurrence of two states lying 0.79 eV and 0.84 eV below the VBM. These two nearly degenerate states correspond to the one surface state and hence are virtually identical in character. From K to *M*, these two states split apart and, at the *M* point, lie 0.56 eV (M_2) and 0.91 eV (M_1) below the VBM. Along the *M*-Γ direction, these two bands gradually approach each other. Charge density contour plots for the occupied surface states at the *K* and *M* points of the SBZ are shown in Fig. 7, together with the corresponding $\rho_{n\mathbf{k}}(z)$. Only one state is presented for the *K* point as the two nearly degenerate states at this symmetry point of the SBZ are virtually identical. It is clear that these occupied surface states are backbond states involving strong bonding between the first-layer silicon atoms and the boron atom at the second-layer site $[B(S_5)]$. The corresponding plots for the Γ-point valence band surface states are shown in Fig. 8(a). The Γ_1 and Γ_2 states are seen to originate from a backbond between the first-layer silicon atoms and the silicon adatom $[\mathrm{Si}(T_4)]$. The Γ_3 surface state, on the other hand, is similar to the occupied surface states at the *K* and *M* points of the SBZ and is associated with the boron atom at the second-layer site $[B(S_5)]$.

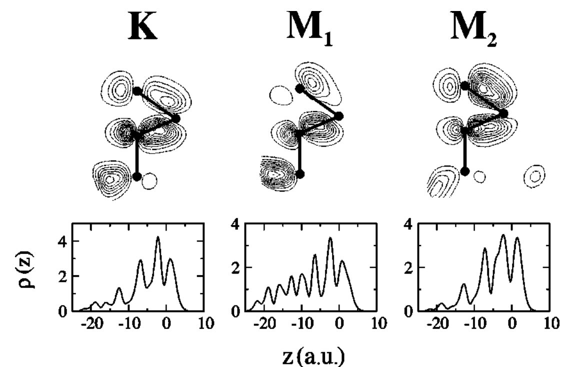

FIG. 7. Charge density and the corresponding $\rho_{n\mathbf{k}}(z)$ for the occupied surface states at the *K* and *M* points of the SBZ for the $B(S_5)$ configuration. The plots for the *K* and M_2 states are for the (0,1,0) plane, while that for the M_1 state is for the (1,1,0) plane.

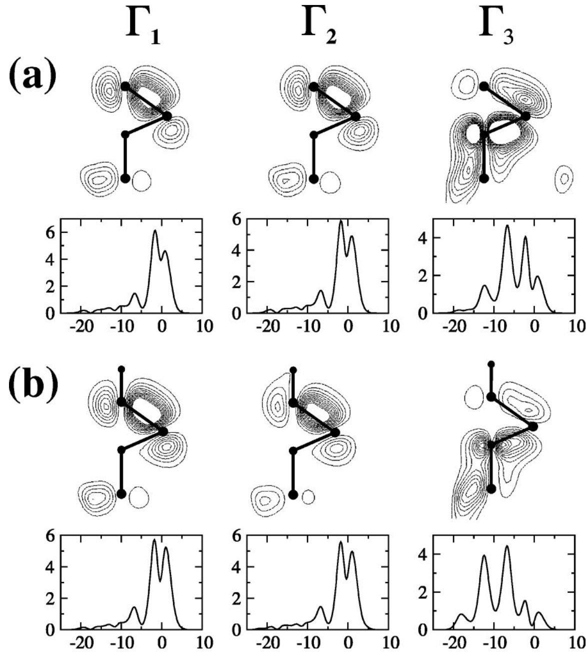

FIG. 8. Charge density and $\rho_{n\mathbf{k}}(z)$ plots for the occupied surface states at the Γ point of the SBZ for the $B(S_5)$ configuration for (a) the clean surface, and (b) the hydrogen chemisorbed surface. The contour plots for the Γ_1, Γ_2 (lower), and Γ_3 (upper) states are for the (0,1,0), (1,0,0), and (1,1,0) planes, respectively.

The experimental data obtained by Higashiyama *et al.*[19] for the valence-band surface-state dispersion of the Si(111)$\sqrt{3}\times\sqrt{3}R30°$-B surface is indicated in Fig. 4 by the open circles and squares. These data values have also been shifted to match the theoretically predicted upper state at the *M* point. Our calculated results are seen to be in excellent agreement with these experimental values. One of the novel features of our calculations is the prediction of two separate surface-state bands (M_1 and M_2) in the vicinity of the *M* point. As stated earlier, an initial photoemission study of the electronic structure of the Si(111)$\sqrt{3}\times\sqrt{3}R30°$-B surface by Kaxiras *et al.*[18] suggested that there was only one occupied surface state below the Fermi energy. The ARUPS studies by Higashiyama *et al.*,[19] however, revealed two occupied surface states with a separation at the *M* point of the SBZ of 0.3 eV. Our theoretical value for this energy difference is 0.35 eV. Our theoretically calculated dispersion for these two surface-state bands is also observed to be in excellent agreement with the experimental data of Higashiyama *et al.*[19]

The valence-band surface states of the Si(111)$\sqrt{3}\times\sqrt{3}R30°$-B surface have also been studied experimentally by Grekh *et al.*[29] Their valence-band data are indicated in Fig. 4 by the open triangles. As for the data of Higashiyama *et al.*, these values have been shifted to match the upper surface state at the *M* point of the SBZ. In agreement with the results of Higashiyama *et al.*, Grekh *et al.* find two occupied surface states at the *M* point with a splitting of 0.30 eV.

The overall correlation between our theoretically predicted valence-band surface states and the results of Grekh *et al.* is observed to be very good. This is particularly evident in the vicinity of the Γ point where our theoretical calculations predict two surface-state bands with a separation of 0.27 eV. While only the upper of these states (Γ_3) appears to have been observed in the experiments of Higashiyama *et al.*, the ARUPS studies of Grekh *et al.* have identified two occupied surface-state bands in the vicinity of the Γ point with a splitting of around 0.31 eV. This is in excellent agreement with our theoretical value of 0.27 eV. The theoretically predicted dispersion of these two surface-state bands is also consistent with the experimental observations. Grekh *et al.* predict that the upper band initially disperses downward along the Γ-*M* direction before increasing in energy. They also predict that the lower band (Γ_1, Γ_2), which is only observed for a small range of **k**, is fairly flat. Both of these features are reproduced by our theoretical calculations.

Grekh *et al.*[29] suggest that the upper band at the Γ point (Γ_3) originates from a backbond of the silicon adatom [$\mathrm{Si}(T_4)$], while the lower state (Γ_1, Γ_2) is associated with bonding between the boron atom in the second layer [$\mathrm{B}(S_5)$] and the surrounding silicon atoms. This suggestion is based primarily on the different behavior of these two bands with hydrogen exposure. The peak in the photoemission spectrum associated with the lower Γ_1, Γ_2 band (denoted by Grekh *et al.* as A_4) was found to be insensitive to the presence of hydrogen while the higher-energy peak Γ_3 (labeled A_3 by Grekh *et al.*) was significantly reduced in intensity. To study this effect we optimized the geometry of the Si(111)$\sqrt{3}\times\sqrt{3}R30°$-B system with a hydrogen atom chemisorbed directly above each $\mathrm{Si}(\mathrm{T}_4)$ adatom. The resulting surface states at the Γ point of the SBZ are shown in Fig. 8, together with the corresponding states for the clean surface. Both the $\rho_{n\mathbf{k}}(z)$ and the charge density plots have been provided for comparision. The $\rho_{n\mathbf{k}}(z)$ for the nearly degenerate lower-lying occupied surface states at the Γ point of the SBZ obtained from our theoretical calculations are seen to be virtually identical, as expected. Both functions are strongly localized in the vicinity of the surface with almost all of the charge lying within the first two surface layers. Moreover, these states remain essentially unaltered following the chemisorption of hydrogen.

The $\rho_{n\mathbf{k}}(z)$ for the upper valence-band surface state at the Γ point of the SBZ (Γ_3) for the clean surface is observed to be much less localized than the lower-lying Γ_1 and Γ_2 states and has its maximum charge in the vicinity of the fourth layer ($z\simeq-7.5$ a.u.). Following hydrogen chemisorption, this state becomes even less localized to the surface region. This is evident from both the $\rho_{n\mathbf{k}}(z)$ plot (which now has a significant peak at $z\simeq-12.5$ a.u.) and the charge density contour plot (which shows a clear shift of charge away from the surface). Our theoretical calculations would thus predict little change in the photoemission intensity of the lower (Γ_1, Γ_2) peak with exposure to hydrogen, but significant change for the upper (Γ_3) peak. This is in agreement with the experimental observations of Grekh *et al.*[29] The nature of these Γ-point surface states, as shown by the plots in Fig. 8, however, is different from that proposed by Grekh *et al.* The latter assumed that states involving adatom backbonds would be more sensitive to hydrogen chemisorption than those associated with bonding to the subsurface boron. Our calcula-

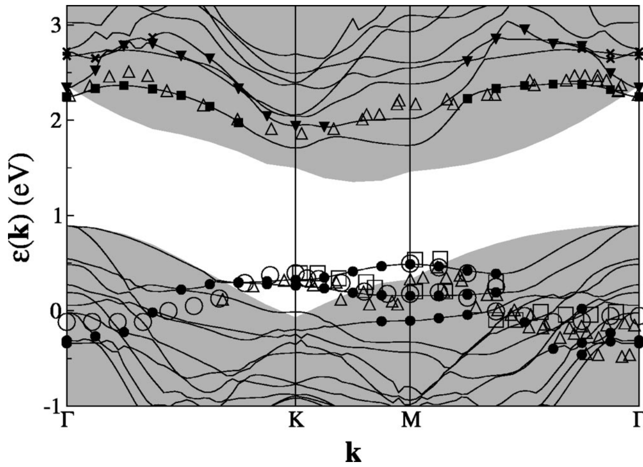

FIG. 9. Electronic structure of the B(T_4) configuration in the vicinity of the VBM. The solid circles, squares, inverted triangles, and crosses indicate the theoretically predicted electronic surface states. The open circles and squares represent the experimental data of Higashiyama *et al.* (Ref. 19) for the B(S_5) configuration. The open triangles indicate the experimental results of Grekh *et al.* for B(S_5) (Ref. 29).

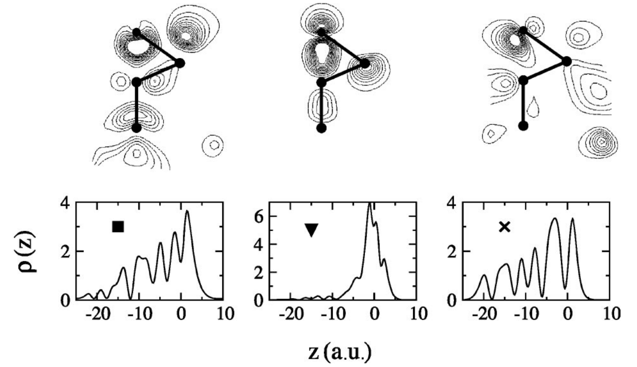

FIG. 10. Plots of the charge density and $\rho_{n\mathbf{k}}(z)$ functions for the theoretically predicted unoccupied surface states for the B(T_4) configuration at the Γ point of the SBZ. $z=0$ corresponds to the position of the first layer atoms in the unrelaxed surface and the bottom silicon layer is at $z=-19.1$ a.u. The charge density contour plots are all for the (0,1,0) plane.

tions have shown, however, that the chemisorption of hydrogen affects the bonding between the subsurface boron and the first-layer silicon atoms, but has almost no effect on the Si(T_4)-Si bonds.

2. Si(111) $\sqrt{3}\times\sqrt{3}$R30 °-B(T_4)

The electronic structure of the B(T_4) configuration was also calculated for comparison. The resulting energy bands are shown in Fig. 9. The theoretical results are indicated by the solid circles (valence band) and by the solid squares, inverted triangles, and crosses (conduction band). The experimental data are those obtained for the B(S_5) surface by Higashiyama *et al.*[19] and Grekh *et al.*[29] The theoretically predicted unoccupied surface states for the B(T_4) configuration are observed to correlate fairly well with the experimental B(S_5) data of Grekh *et al.*[29] In contrast to the B(S_5) case, however, we can no longer identify any well-defined unoccupied surface states in the vicinity of the *M* point. We have observed three different types of low-lying unoccupied surface states for the B(T_4) configuration. The natures of these three states (indicated by the solid squares, inverted triangles, and crosses) are illustrated in Fig. 10 where we have plotted the $\rho_{n\mathbf{k}}(z)$ and the corresponding charge density distributions for each of these states at the Γ point of the SBZ. One of the states (inverted trangles) is seen to be strongly localized in the surface region with its main peak lying below the first layer silicon atoms. The other two states (squares and crosses) are less localized and have strong peaks lying above the first layer silicon atoms.

The basic distribution of the occupied surface states, as represented by the black circles, is seen to be very similar to that for the B(S_5) configuration. As before, there are two nearly degenerate states at the *K* point and a single surface-state band which decreases in energy along the *K*-Γ direction of the SBZ. From *K* to *M* we observe a splitting into two bands with a separation at the *M* point of 0.33 eV. This is very similar to the value of 0.35 eV that we obtained for the B(S_5) topology. For B(T_4) we observe the occurrence of a third surface state in the vicinity of the M-point. Such a state was not observed for B(S_5). The other obvious difference in the valence-band structure occurs at the Γ point where we now observe only a single band consisting of two nearly degenerate surface states approximately 1.3 eV below the VBM.

3. Si(111) $\sqrt{3}\times\sqrt{3}R30$ °-Al, Si(111) $\sqrt{3}\times\sqrt{3}R30$ °-Ga, and Si(111) $\sqrt{3}\times\sqrt{3}R30$ °-In

Finally, we have compared our calculated B(S_5) and B(T_4) electronic structures with the band structures obtained for the Si(111) $\sqrt{3}\times\sqrt{3}R30°$-Al, -Ga and -In surfaces by other researchers. We have found that the distributions of the adatom-induced surface states of these T_4 adatom chemisorbed structures are very similar to those presented in Figs. 4 and 9 for the B(S_5) and B(T_4) topologies, respectively. All of the electronic structures are observed to split into two surface-state bands near the *M* point. The magnitude of the energy splitting at the *M* point varies, however, from one topology to another. The Al(T_4), Ga(T_4), and In(T_4) band structures show only one surface state band at the Γ point of the SBZ. This is consistent with both our B(T_4) electronic structure and experiment.

IV. SUMMARY

The plane-wave pseudopotential DFT method, FHI98MD, has been used to optimize the geometry of the Si(111) $\sqrt{3}\times\sqrt{3}R30°$-B($S_5$) configuration. The resultant geometry has been found to be in excellent agreement with the recent experimental results of Baumgartel *et al.*[25] Using the FHI98MD program we have also calculated the band structure for the B(S_5) configuration. By carefully analyzing the nature of the wave functions in the vicinity of the Fermi energy, we have been able to identify the surface states along the various symmetry directions of the SBZ. We have found that there

are two surface-state bands below the Fermi energy with a splitting at the *M* point of 0.35 eV. This prediction and the overall dispersion of the surface-state bands are in excellent agreement with the ARUPS data of Higashiyama *et al.*[19] and Grekh *et al.*[29] Our theoretical calculations have also predicted the occurrence of two surface-state bands at the Γ point of the SBZ. Both the dispersion of these surface states and their sensitivity to hydrogen chemisorption were found to be in good agreement with the experimental data of Grekh *et al.* The lower surface-state band was found to originate from bonding between the silicon adatom $[\mathrm{Si}(T_4)]$ and the first-layer silicon atoms, while the upper band involved bonding between the boron atom in the second layer $[\mathrm{B}(S_5)]$ and its neighboring silicon atoms. Only the latter of these two surface states was found to be significantly affected by the chemisorption of hydrogen on the Si(111) surface.

The electronic structure of the $\mathrm{Si}(111)\sqrt{3}\times\sqrt{3}\mathrm{R}30°\text{-}\mathrm{B}(T_4)$ configuration was also calculated. The nature and dispersion of the surface-state bands was found to be very similar to that of the $\mathrm{B}(S_5)$ configuration. In agreement with the $\mathrm{Al}(T_4)$, $\mathrm{Ga}(T_4)$, and $\mathrm{In}(T_4)$ chemisorption systems, however, the $\mathrm{B}(T_4)$ configuration was found to have only one surface-state band at the Γ point of the SBZ, compared to two for $\mathrm{B}(S_5)$.

ACKNOWLEDGMENTS

One of us (H.Q.S.) would like to thank the Australian Government and the University of Newcastle for financial support.

*Electronic address: phpvs@alinga.newcastle.edu.au

[1] J.P. LaFemina, Surf. Sci. Rep. **16**, 133 (1992); W. Monch, *Semiconductor Surfaces and Interfaces*, Springer Series in Surface Science Vol. 26 (Springer-Verlag, Berlin, 1993); H.N. Waltenburg and J.T. Yates, Chem. Rev. **95**, 1589 (1995).

[2] R.I.G. Uhrberg and G.V. Hansson, Crit. Rev. Solid State Mater. Sci. **17(2)**, 133 (1991).

[3] S. Kono, Surf. Rev. Lett. **1**, 359 (1994).

[4] G.V. Hansson, R.Z. Bachrach, R.S. Bauer, and P. Chiaradia, Phys. Rev. Lett. **46**, 1033 (1981).

[5] G.V. Hansson, R.Z. Bachrach, and R.S. Bauer, J. Vac. Sci. Technol. **18**, 550 (1981).

[6] R.I.G. Uhrberg, G.V. Hansson, J.M. Nicholls, P.E.S. Persson, and S.A. Flodstrom, Phys. Rev. B **31**, 3805 (1985).

[7] T. Kinoshita, S. Kono, and T. Sagawa, Phys. Rev. B **32**, 2714 (1985).

[8] T. Kinoshita, S. Kono, and T. Sagawa, Solid State Commun. **56**, 681 (1985).

[9] T. Kinoshita, S. Kono, and T. Sagawa, Phys. Rev. B **34**, 3011 (1986).

[10] T. Kinoshita, H. Ohta, Y. Enta, Y. Yaegashi, S. Suzuki, and S. Kono, J. Phys. Soc. Jpn. **56**, 4015 (1987).

[11] J.M. Nicholls, P. Martensson, G.V. Hansson and J.E. Northrup, Phys. Rev. B **32**, 1333 (1985).

[12] J.M. Nicholls, B. Reihl, and J.E. Northrup, Phys. Rev. B **35**, 4137 (1987).

[13] J.E. Northrup, Phys. Rev. Lett. **53**, 683 (1984).

[14] J. Zegenhagen, J.R. Patel, P. Freeland, D.M. Chen, J.A. Golovchenko, P. Bedrossian, and J.E. Northrup, Phys. Rev. B **39**, 1298 (1989).

[15] R.L. Headrick, I.K. Robinson, E. Vlieg, and L.C. Feldman, Phys. Rev. Lett. **63**, 1253 (1989).

[16] P. Bedrossian, R.D. Meade, K. Mortensen, D.M. Chen, J.A. Golovchenko, and D. Vanderbilt, Phys. Rev. Lett. **63**, 1257 (1989).

[17] I.W. Lyo, E. Kaxiras, and Ph. Avouris, Phys. Rev. Lett. **63**, 1261 (1989).

[18] E. Kaxiras, K.C. Pandey, F.J. Himpsel, and R.M. Tromp, Phys. Rev. B **41**, 1262 (1990).

[19] K. Higashiyama, S. Yamazaki, H. Ohuki, and H. Fukutani, Solid State Commun. **87**(5), 455 (1993).

[20] M. Bockstedte, A. Kley, J. Neugebauer, and M. Scheffler, Comput. Phys. Commun. **107**, 187 (1997).

[21] D.R. Hamann, Phys. Rev. B **40**, 2980 (1989).

[22] We are grateful to Martin Fuchs for providing us with his hydrogen pseudopotential.

[23] V.D. Zavodinsky, I.A. Kuyanov, and E.N. Chukurov, J. Vac. Sci. Technol. A **17**(5), 2709 (1999).

[24] S. Wang, M.W. Radny, and P.V. Smith, Phys. Rev. B **59**, 1594 (1999).

[25] P. Baumgartel, J.J. Paggel, M. Hasselblatt, K. Horn, V. Fernandez, O. Schaff, J.H. Weaver, A.M. Bradshaw, D.P. Woodruff, E. Rotenberg, and J. Denlinger, Phys. Rev. B **59**, 13 014 (1999).

[26] S. Wang, M.W. Radny, and P.V. Smith, J. Phys.: Condens. Matter **9**, 4535 (1997).

[27] H. Huang, S.Y. Tong, J. Quinn, and F. Jona, Phys. Rev. B **41**, 3276 (1989).

[28] R.D. Meade and D. Vanderbilt, Phys. Rev. B **40**, 3905 (1989).

[29] T.M. Grehk, P. Martensson, and J.M. Nicholls, Phys. Rev. B **46**, 2357 (1992).